공학석사학위논문

Design for Flapping Wing Micro Vehicle Using 6-Bar Linkage Mechanism

6절 링크를 이용한 날갯짓 초소형 비행체 설계

2016년 2월

서울대학교 대학원

기계항공공학부

전 재 혁

Design for Flapping Wing Micro Vehicle Using 6-Bar Linkage Mechanism

6절 링크를 이용한 날갯짓 초소형 비행체 설계

지도교수 신상준

이 논문을 공학석사 학위논문으로 제출함

2016년 2월

서울대학교 대학원

기계항공공학부

전 재 혁

전재혁의 석사학위논문을 인준함

2016년 2월

위 원 장 김 종 안 (인)

부 위 원 장 신 상 준 (인)

위 원 이 관 중 (인)

Abstract

Design for Flapping Wing Micro Vehicle Using 6-Bar Linkage Mechanism

Jaehyeok Jeon

Mechanical and Aerospace Engineering

The Graduate School

Seoul National University

Recently, there occurs rise and growth of the research on the flapping wing vehicles by mimicking the biological motion. Its result is so-called the Flapping Micro Aerial Vehicle (FWMAV). In this thesis, design requirements for FWMAV were established by using an analytical tool and unsteady blade element theory (UBET). Based on the present FWMAV design requirements, flapping wing mechanism using a six-bar linkage was devised. Moreover, the present mechanisms were analyzed by using the flexible multi-body dynamic analysis to ensure its structural robustness. By completing such procedure, behavior of the present mechanism was estimated. Then, detail design was conducted. Currently, structural analysis regarding the present mechanism was conducted under the flapping operation in vacuum. And the resulting von-Misses stresses in the linkage were designed to be smaller than the yield stress of the chosen material. After that, detail design and experiment of the present FWMAV were conducted for validating the performance, such as aerodynamic force, flapping frequency and flapping amplitude.

Keywords: Flapping wing, Multi-body dynamic analysis, Six-bar linkage

Student Number: 2014-20667

Table of Contents

List of Figures

List of Tables

I. Introduction

Flapping wing micro aerial vehicle (FWMAV) has been developed during the last few decades with considerable growth of its research. Design of the FWMAV generally is performed through an idea inspired by the nature flyers by mimicking their biological feature, as shown in Fig. 1.1. The reason for studying the nature flyer is that they can hover flight unlike a fixed-wing MAV's and are more efficient than those of a rotary-wing MAV's [8]. Using these advantages, FWMAV is capable of conducting various tasks. Especially the insect-mimicking FWMAV operates in low Reynolds number aerodynamic environment. Its flight control is performed by using a couple of the wings with high flapping frequency and large flapping amplitude. As a result, such FWMAV's may have complicated mechanism to be operate under such conditions. Moreover, FWMAV's have no tail wing. To control their body, FWMAV's need to use both side of the flapping wing motions. Nowadays many methods for a stable flight are being studied.

Figure 1.1 Nature flyer

There exist certain kinds of flapping mechanism. One of those is Nano Hummingbird [1] developed by AeroVironment, Inc as shown Fig 1.2. Its driving component was made up of string which enables the wings to move simultaneously. Also, the string mechanism takes a small space because it is not a complicate structure whose total weight is only 19g including the 2.47g of flapping mechanism. Nano hummingbird has 165mm wing span wing 74mm wing length and flapping frequency is 30Hz. It is one of the most advanced vehicles which can hover, do backward and forward flights. The flight speed of this FWMAV is 6.7m/s.

Figure 1.2 Nano hummingbird developed in AeroVironment [1]

Robobee [3] developed in Harvard University is the smallest vehicle using piezoelectric bimorph actuator for its driving component as shown in Fig 1.3. A plastic joints are used to flapping hinge. Moreover, it can control the each wing separately for changing the body position. The mechanism also consists of a simple structure. Thus, the total weight of the FWMAV is merely 80mg. To fly that vehicle, 120Hz flapping

frequency is required with 30mm wingspan. However, Robobee needs an external power source yet because of the micro piezoelectric actuator requires high voltage.

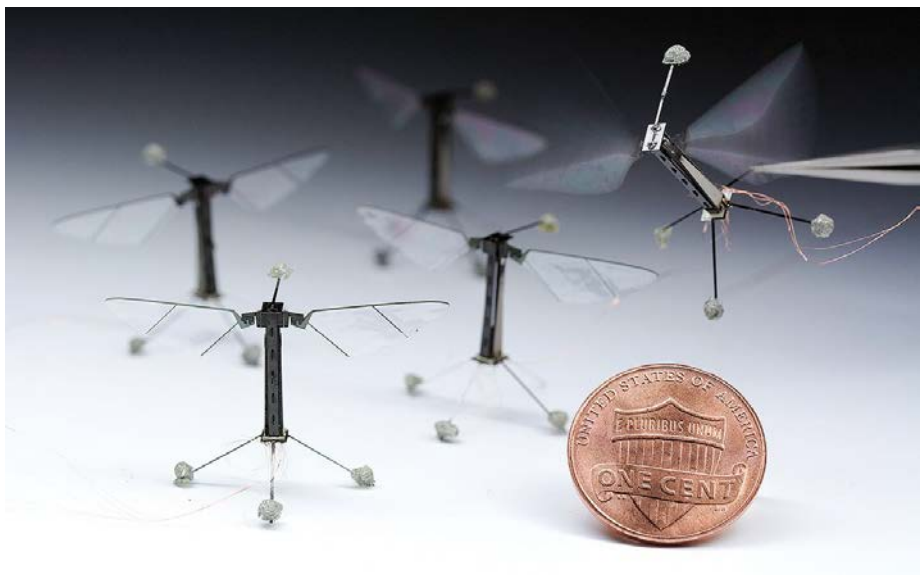

Figure 1.3 Robobee developed in Harvard University [3]

Delfly [9] developed in Delft University is using four bar linkage in Fig.1.4. Four bar linkage is a simple structure and widely used for decades because it`s robustness. However, this mechanism produces small flapping amplitude. Defly`s flapping amplitude is 48° which appropriates for ornithopter, like birds. The total weight of Defly is 17g. To lift the body, the flapping frequency is 14Hz with 280mm wing span. In addition, Defly used clap-and-fling mechanism having more circulation to get an aerodynamic advantage. By this mechanism, it makes lift force with relatively easy.

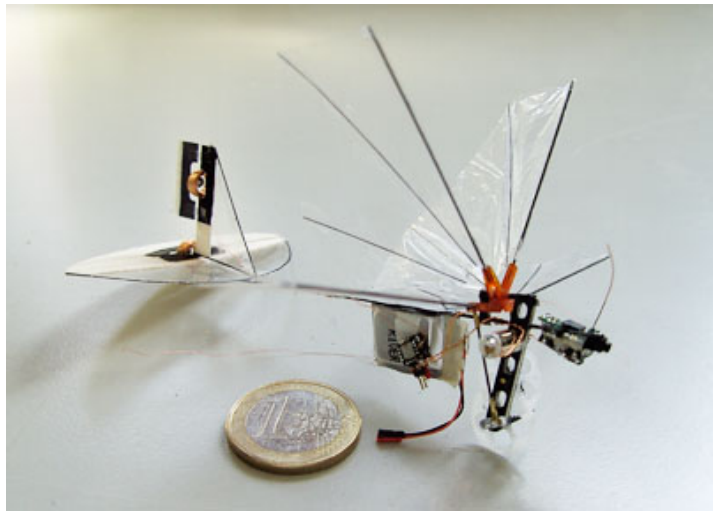

Figure 1.4 Defly developed in Deft University [9]

BionicOpter [10] by Festo looks like dragonfly. It has four wings to generate lift and control force. The flapping mechanism consist of a slider having linear transition located in wing root and four motors in each wing. The flapping amplitude is about 80°~130°. It is relatively small compared with insect flyers. It`s total weight is 175g and wingspan is 640mm. To lift the body, the flapping frequency is 15~20Hz.

Figure 1.5 BionicOpter developed in Festo [10]

In addition, a few vehicles, such as Golden snitch [4] by Tamkang University and Robotic hummingbird by Bruxelles University [6], adopted typical mechanical linkage for flapping wing movement.

The insect-mimicking FWMAV's need to generate control forces, i.e., pitching, yawing, and rolling moments, by using a couple of wings. This suggests that aerodynamic forces generated in both wings should be unbalanced [6]. Based on such physical characteristics, there exist several control mechanisms available. First, Nano Hummingbird uses wing twisting and wing rotating mechanism [1]. Nano hummingbird`s wing is a passively rotated at the leading edge. Thus, during the flapping motions, aerodynamic forces tilt the wing plane. The wing rotating mechanism is restrict this wing motion, as shown Fig 1.6. By this method, the wing`s aerodynamic forces, such as lift and drag, are modified to generate the control force to change the body position. The wing twisting mechanism changes the tension of the each wing separately by tight or loose-membrane as shown in Fig. 1.7. This motion is obtained by modifying the trailing edge and it generate the different aerodynamic forces on each wing.

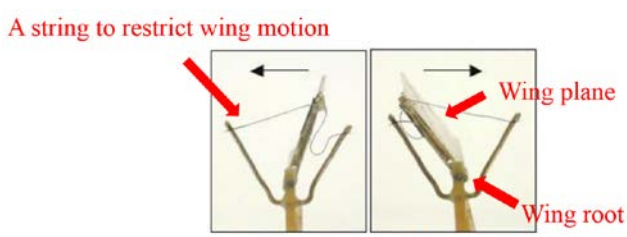

Figure 1.6 Wing rotating mechanism by Nano hummingbird [1]

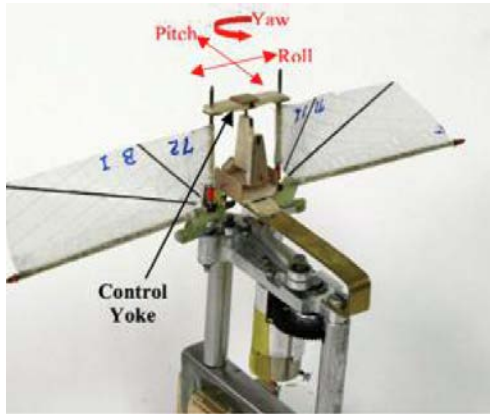

Figure 1.7 Wing twisting mechanism by Nano hummingbird [1]

Next, BionicOpter [10] by Festo modifies the flapping frequency of each wing separately and the direction of the flapping plane of each wing to generate such unbalanced aerodynamic force as depicted Fig. 1.8. BionicOpter also control its body by change the head and tail.

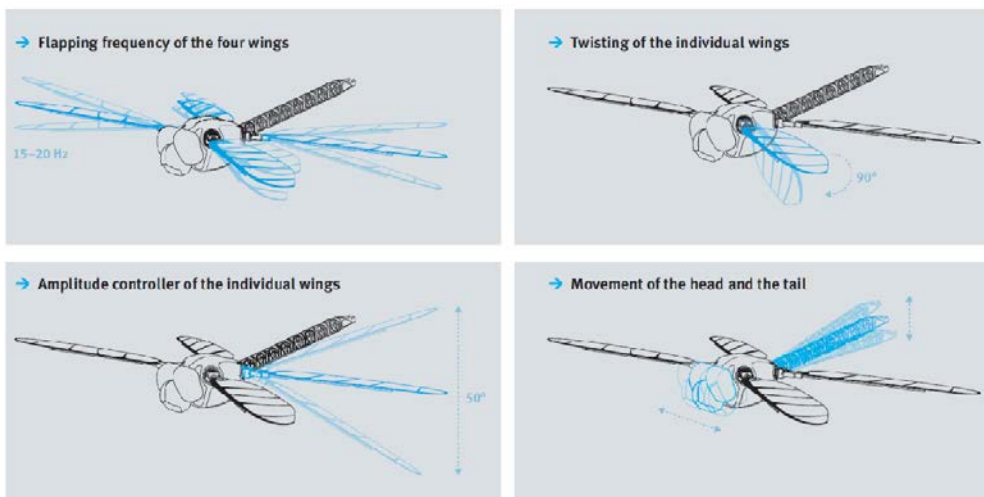

Figure 1.8 Control mechanism of BionicOpter [10]

On the other hand, robotic hummingbird by Bruxelles University varies the position of kinematic joints to change the flapping amplitude and offset of the flapping plane, as shown Fig. 1.9 [6]. Movement of the flapping amplitude change the wing`s lift and drag and rotation of the flapping plane generate the movement of the aerodynamic center on the wing. Consequently, it changes the moment of the body. By this two methods, robotic hummingbird can modulate its body position to want direction.

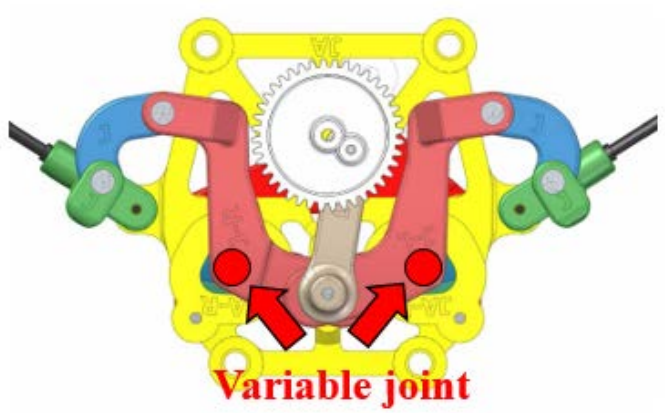

Figure 1.9 Control mechanism of Robotic Hummingbird [6]

However, several of mechanisms as mentioned earlier need a lot of space because of their large driving or control components. And, modifying the trailing edge required experimental verification and aerodynamics database to induce reasonable performance. Also, significant collaboration with analytical design has been required among the design procedures.

In this thesis, a six-bar linkage mechanism is designed. The present mechanism requires small-size driving component through the two separated kinematics steps using six-bar linkage characteristic. And the control wing motions are generated easily from a small position change of the joints. Also, the kinematics and structural analysis may give a more realistic result for the design. By using the fundamental analysis using unsteady blade element theory (UBET) [2], certain design requirements will be established. Then, design for the flapping mechanism using mechanical linkage will be performed. In order to predict the structural robustness of the present mechanism, analysis using RecurDyn, a multi-flexible body dynamic analysis, will be performed. In the present mechanism, wings will be connected to the mechanical linkage and not be directly connected to the joint. Thus, it is possible to obtain the sufficient flapping amplitude and control the flapping kinematic by varying the joint location. Currently, using the results of the structural analysis, detailed design of the present mechanism will be performed. Finally, experiment on the present mechanism will be conducted for validating the performance, such as aerodynamic force, flapping frequency and flapping angle.

II. Design Procedure

In the previous studies, kinematic analysis using multi-body dynamics was not employed in the design procedure of the FWMAV, although it was capable of providing a precise design result. In this thesis, design procedure which considers the multi-body dynamics analysis is introduced as shown in Fig 1. Design procedure is divided into 5 stages from the conceptual design stage to the modification and supplement stage. The first stage is the conceptual design. In this stage, the idea is developed with the design requirements. Then, the developed idea is embodied in three-dimensional CAD shape before the multi-flexible body dynamic analysis is conducted. By using this three-dimensional CAD design, multi-flexible body dynamic analysis utilizing commercial software, RecurDyn, is performed to check the possibility of fabrication by understanding the design parameters and execution error. However, external aerodynamic loads due to the flapping wing will not be considered in the present analytical process yet. In the future, detailed aerodynamic loads will be predicted. Then, it will be coupled with the structural analysis in order to improve a precision of the present design process. After that, performance of the conceptual design is evaluated regarding whether to go to next stage or return to conceptual design stage. If a designed mechanism has unexpected problems in this stage have, it has to return to concept design stage again. Next stage is the fabrication and experiment. At this stage, conceptual design is realized with by applying the actual components, such as DC motor,

gears, brass bearing, pins and body frame. After the fabrication, FWMAV`s performance is evaluated by test bed such as aerodynamic force, flapping conditions and design requirements. In this stage, flapping wing trajectory is measured by high-speed camera. And forces and moments are measured by load-cell. If there exist any problem, modification and supplement will be need. Through this procedure, the flapping mechanisms will be optimized and possess robustness.

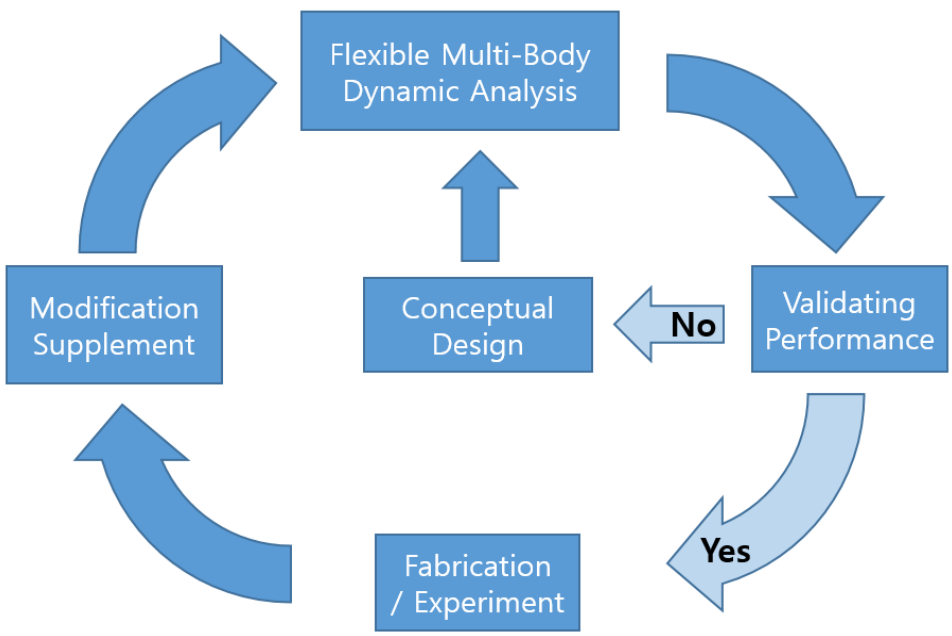

Figure 2.1 Diagram of design procedure

III. Design Requirement

In this section, preliminary design requirements will be established. First, the wing span was determined to be 150mm by referring to the definition of the general FWMAV. And then, its gross weight was assumed to be 20g by considering the off-the-shelf products, such as electric motor, servo motor, joint pin, and so on. After that, appropriate flapping amplitude and actuation frequency which create sufficient lift were estimated by using the UBET prediction [7]. UBET is the unsteady blade element theory which is based on the quasi-steady aerodynamics. In the present UBET analysis, wing mass and center of gravity were chosen to be 0.1g and 0.1% respectively, along the chord length, respectively. And three kinds of the wing planform were considered, i.e., rectangular, elliptic, and insect-like wings. Configurations of the wings are illustrated in Fig. 3.1.

According to the results obtained by the UBET analysis, flapping stroke amplitude and actuation frequency need to be greater than 150° and 37Hz, respectively, to obtain a sufficient lift for the gross weight, 20g. Table 3.1 shows the results with respect to these wing planforms. Now, fundamental design requirements for the present FWMAV were determined. The results are summarized in Table 3.2.

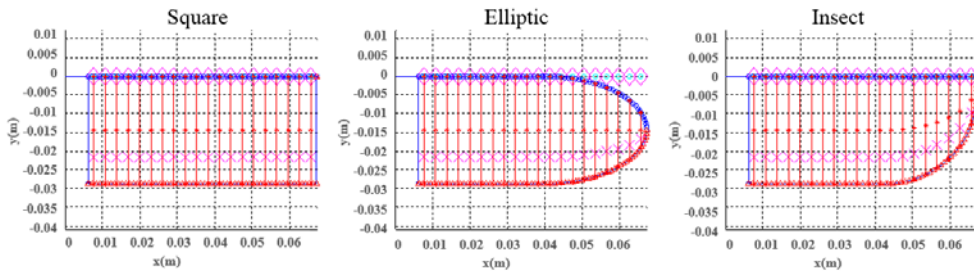

Figure 3.1 Three wing planform configurations

Table 3.1 UBET results at flapping amplitude of 150° and frequency of 37Hz

Planform	Square	Elliptic	Insect
Thrust (N)	0.236	0.19	0.20
Area of single wing (mm^2)	1761.3	1584.5	1627.211
Thrust/Area of 1 wing (N/m^2)	67.13	60.10	61.54

Table 3.2 Preliminary design requirements for the present FWMAV

Wingspan	Weight	Flapping Amplitude	Flapping Frequency
150mm	20g	150°	37Hz

IV. Flapping Mechanism

The present driving components consist of DC motor, gears, brass bearing and linkages. To generate the flapping motion, revolutionary motion of the motor must be transformed to reciprocating angular motion. In the present mechanism, certain six-bar linkage is employed to provide a combination of two separated kinematics. One mechanism nearby the input link is the first step. In the first step, through this input link the DC motor power is delivered to six-bar linkage. The mechanism is the crank-slider mechanism which consists of four-bar linkage with one sliding joint and creates back and forth motion. However, the crank-slider mechanism is asymmetric mechanism which makes a difference slider speed between the forward and return stroke, so-called quick return mechanism. If the flapping mechanism only consist of the four bar linkage, motor rotation makes asymmetric reciprocating flapping motion. To reduce the asymmetric characteristic of the crank-slider, an alternate step mechanism is required. The second step nearby the wing consists of the crossed four-bar link which compensates the asymmetry of the first step four-bar linkage. Moreover, this second step is capable of amplifying the crank-slider motion in the first step as depicted in Fig.4.1. This suggests that the final flapping angle can be increase further. By using this mechanism, the designed flapping amplitude is 160°. It satisfy the target amplitude because it is larger than those of design requirement. Six bar linkage mechanism has many revolute joints. The main purpose of the revolute joints is to support the structure load.

Besides, the joints are strongly related with kinematics of wing motion. Thus, an advantage of using six bar linkage is that the flapping kinematics on the both wings are easily modified by the joint position change. Also, the small displacement of joint position has a strong influence on flapping amplitude because the wing kinematics is sensitive to joints position. Using such mechanism, it is possible to minimize the size of the driving components and implement the desired control capability at the same time. To reduce the weight of the frames used in the present mechanism, composite material such as epoxy glass laminate will be used.

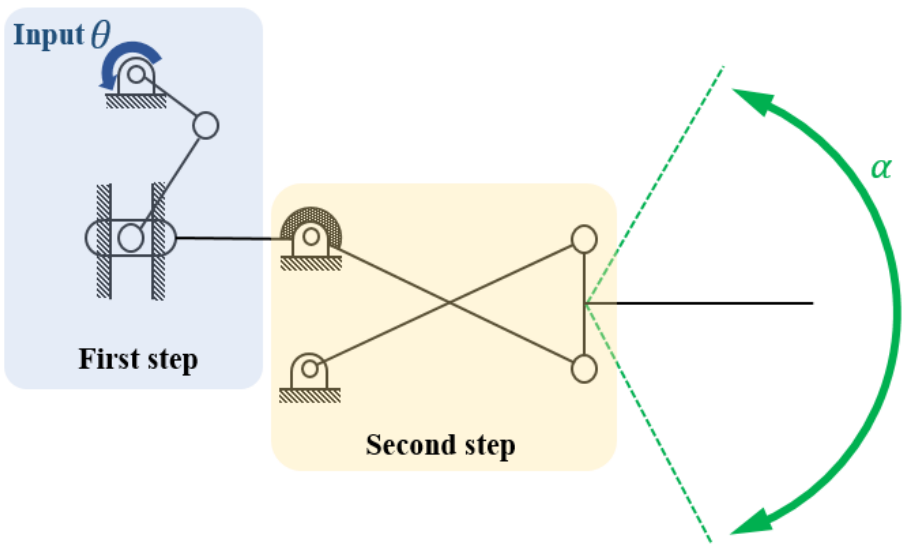

Figure 4.1 Diagram of the two step flapping mechanism

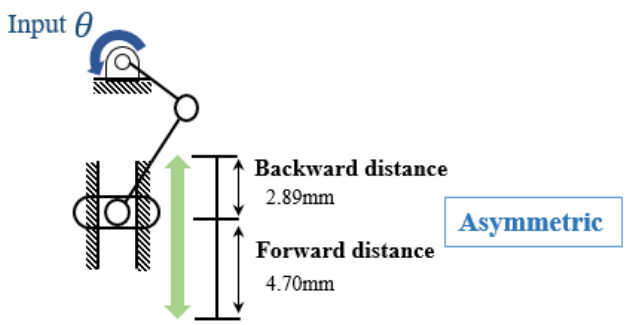

Figure 4.2 Diagram of the first step

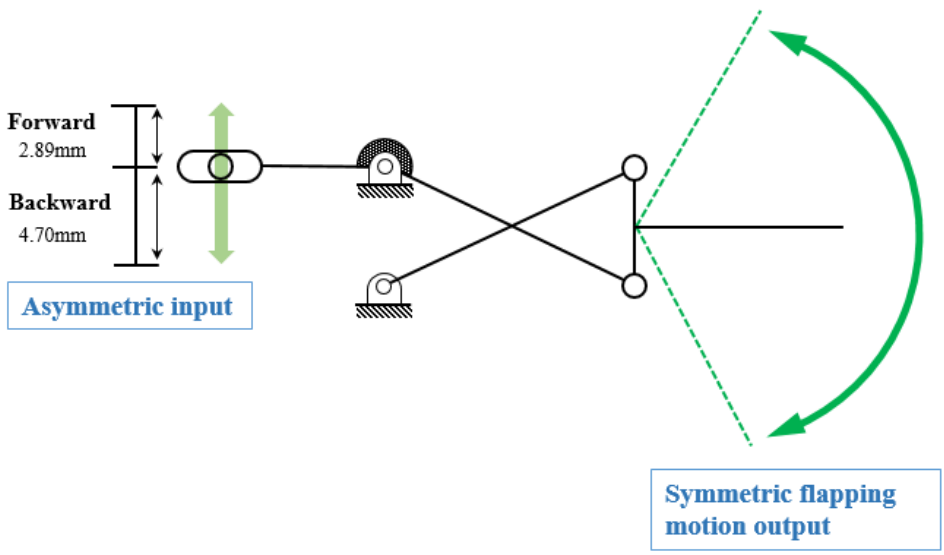

Figure 4.3 Diagram of the second step

4.1 Kinematics of the present flapping mechanism

As mentioned earlier, the present six-bar linkage uses the following two steps to create the flapping motion. Here, the kinematics of linkages is analyzed to predict the motion. The first mechanism of the six-bar linkage can be expressed by taking the geometry and angular motion of the frames into account as follows.

$$\theta_4 = \frac{\sqrt{r_3^2 - (r_2 \sin\theta_1)^2} + r_2 \cos\theta_1 - r_1}{r_4} \quad \textbf{(1)}$$

Here, θ_1 is the input angle by the motor rotation, θ_4 is the initial angle of the second mechanism. The first stage in the crank-slider mechanism is capable of generating displacement at point P_3 by the motor rotation. Then, joints rotation in the second mechanism can be derived from the equation of the four-bar linkage. The resulting formulas can be expressed by these follows.

$$\theta_6 = \cos^{-1}\left(\frac{C}{\sqrt{A^2 + B^2}}\right) + \tan^{-1}\left(\frac{B}{A}\right) \quad (2)$$

$$\theta_5 = \sin^{-1}\left(\frac{r_6 \sin\theta_4 - r_8 \sin\theta_6}{r_7}\right) \quad (3)$$

$$\theta_7 = \cos^{-1}\left(\frac{r_6^2 + r_7^2 - \left(\sqrt{(-r_5 + r_8\cos\theta_6)^2 + (r_8 \sin\theta_6)^2}\right)^2}{2 r_6 r_7}\right) \quad (4)$$

Here, A , B and C are determined by the following geometrical consideration for the linkages.

$$A = -2(r_6 r_8 \cos\theta_4) + 2r_5 r_8$$
$$B = -2r_6 r_8 \sin\theta_4 \qquad (5)$$
$$C = r_7^2 - r_6^2 - r_8^2 - r_5^2 - 2r_5 r_6 \cos\theta_4$$

By completing those procedures, it will be possible to predict kinematics of the linkages accurately. Flapping stroke amplitude in the present mechanism is obtained by the complicated linkage motion as shown in Fig. 4. The bending angle of the linkage r_8 is expressed γ . The first mechanism made of the crank-slider is capable of transforming the motor rotation into the straight-line motion. But such motion output is not symmetric as mentioned earlier. The second mechanism is made of the four-bar linkage. It increases the amplitude of the motion in the first mechanism. The combination of these two stages generates total flapping amplitude. Thus, the flapping amplitude in this mechanism is defined by the sum of joint rotation at Point P_4 in the first step and at Point P_5 in the second step. The dimension of the driving components were satisfactory with respect to the design requirements. All the driving components except for gear and motor are fabricated by CNC cutting machine having 0.005mm accuracy. Also, 1mm-diameter pin is used at each joint. Therefore, the minimum possible length of the linkage was found to be 2mm. The dimensions of each linkage were determined as shown in Table 4.4.

Table 4.1 Dimensions of the linkage components

Linkage	r_1	r_2	r_3	r_4	r_5	r_6	r_7	r_8	γ
Length (mm)	6.91	3.75	7.86	3.5	3.5	8	4.5	9	30°

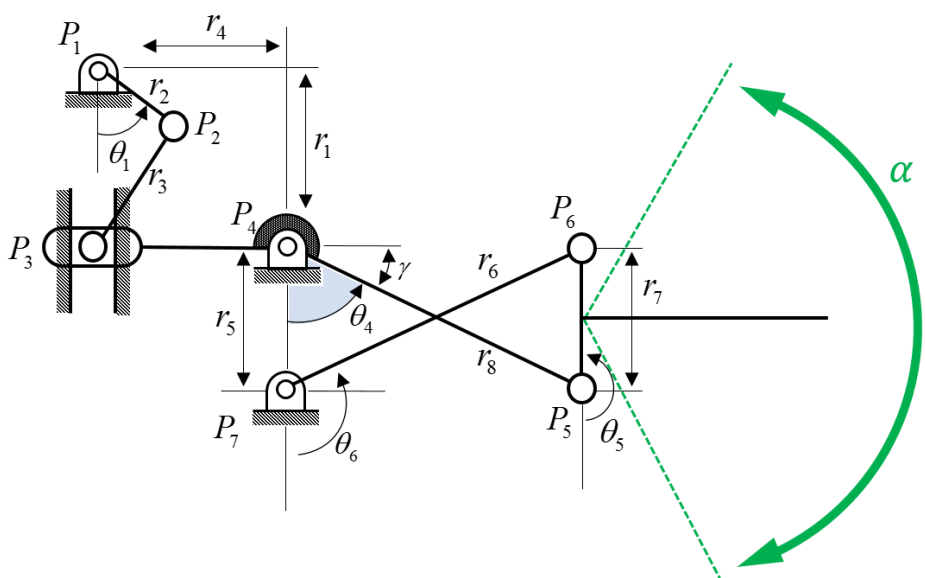

Figure 1.4 Kinematic diagram of the present six-bar linkage

V. Control Mechanism

5.1 Conceptual design of the control mechanism

In the insect-mimicking FWMAV, aerodynamic difference between both wings induces unbalanced moments. Therefore, the FWMAV can change its wing position. Figure 5.1 illustrates the right-hand side of the wing and describes the joint motion along θ- and r-direction at P_7. This joint with two degrees of freedom can modify the flapping trajectory, α and β. The value of α is flapping amplitude and β is alteration of the center line of the flapping amplitude. To estimate the influence with respect to the motion of the joint P_7, the wing trajectory is analyzed by using kinetic analysis. This analysis is conducted with both vacuum and perfect revolute joint condition. Figure 5.2 shows the trajectory curves of the flapping amplitude, α, with respect to the variations of the joint P_7 according to θ- and r- direction. Figure 7 shows the trajectory curves regarding the rotation angle of flapping center line with respect to the variations, θ and r. When the joint rotation angle θ is 55° or 230°, the flapping stroke amplitude maintains its neutral flapping amplitude 160°, as depicted in Fig. 5.2. But the rotation of the flapping center line is changed to the positive or negative value as depicted in Fig.5.3. It means that the flapping trajectory will rotate by an amount of β with constant $\alpha = 160^\circ$. This result is regardless of the joint displacement r. By using such mechanism, the flapping stroke plane will be varied in clockwise or counter-clockwise. But, the same flapping stroke amplitude will be

maintained. Thus, the aerodynamic center of the wing will be changed. Consequently, the resulting moment will become changed. By applying such mechanism for each wing, it will be possible to generate yawing and pitching moment on the vehicle. Moreover, when the joint rotation angle θ is 175° or 353°, the rotation of flapping center line keeps its neutral position $\beta = 0^{\circ}$ regardless of the joint displacement, r, as shown in Fig. 5.3. Simultaneously, the flapping stroke amplitude will become the positive or negative value according to the joint displacement, r, as shown in Fig. 5.2. By using this mechanism, it will be possible to create either increase or decrease the flapping stroke amplitude. This motion enforces the different amount of lift force on the wings, generated along a perpendicular axis to the stroke plane. As a result, it is possible to generate rolling moment on the vehicle. The magnitudes of both α and β are changed with respect to r. In the present control mechanism, the joint displacement, r, is chosen to be 0.8mm which leads to the maximum amount regarding the changes of the flapping stroke.

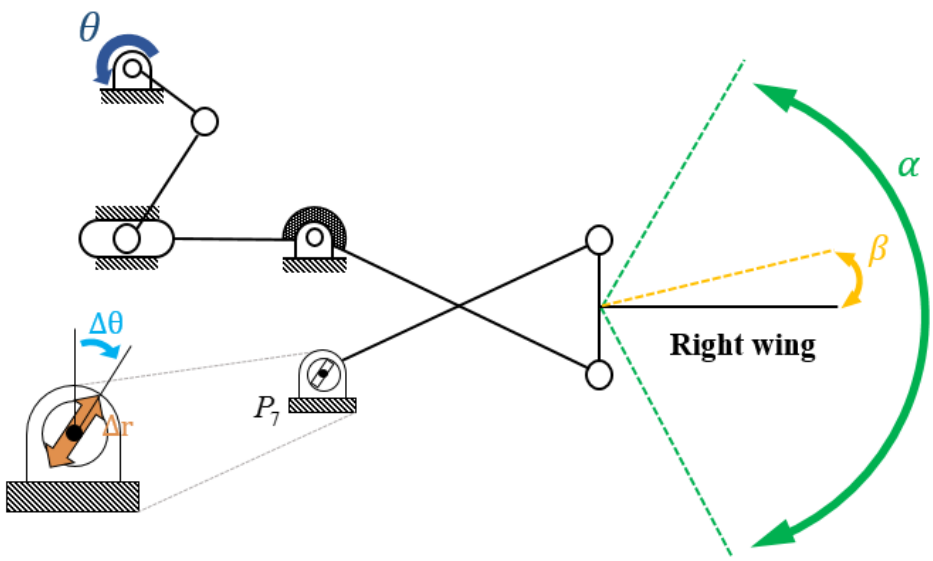

Figure 5.1 Kinematic diagram of the moving joint on the right wing

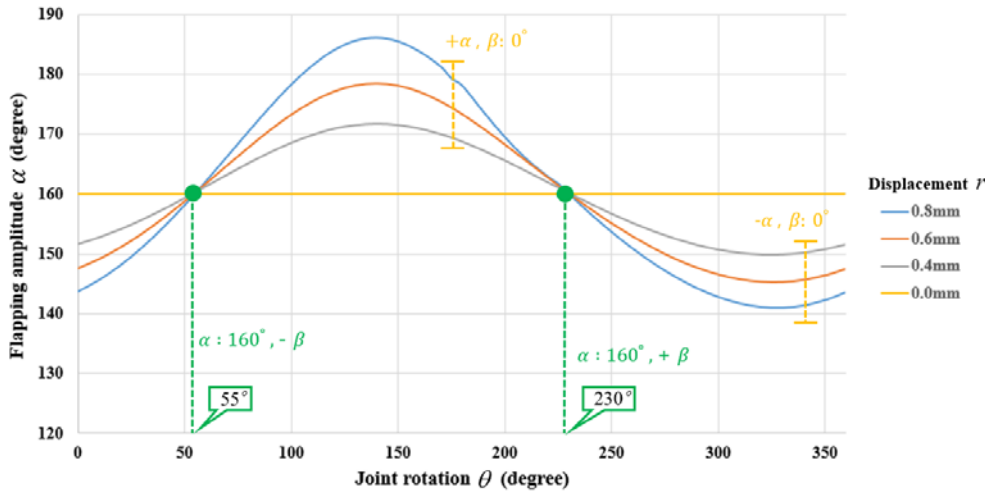

Figure 5.2 Trajectory curve of the flapping amplitude

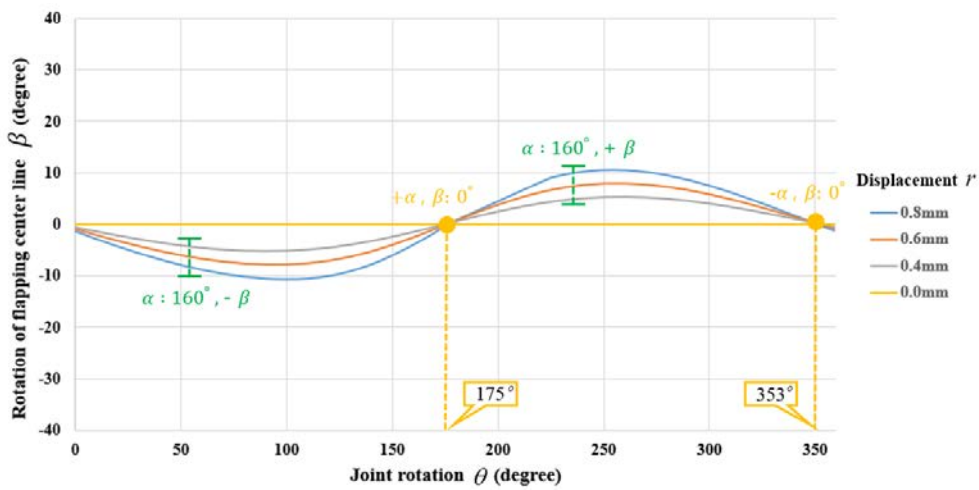

Figure 5.3 Trajectory curve of the rotation of flapping center line

5.2 Pitching, rolling, and yawing motion

In the previous section, the possibilities of changing the flapping amplitude α and flapping center line β are confirmed. Combining this two kinds of wing motion, aerodynamic center will be changed. And then, pitching, yawing and rolling motions are embodied as mentioned below.

In order to generate the pitching moment, both wings remain their flapping amplitude $\alpha = 160^{\circ}$ And, the center line of the flapping stroke is rotated symmetric by the same magnitude, β. The relevant situation is illustrated in Fig. 5.4. In the figure, the aerodynamic center of both wings is segregated from the vehicle`s center of gravity. Aerodynamic center of each wing come together in forward or backward direction from the body. Thus, it leads to nose up or down.

Next, yawing moment can be generated by the unsymmetrical motion of the wings. Both wings remain their flapping amplitude $\alpha = 160^{\circ}$and rotated each wing in reverse direction, as shown in Fig. 5.5. Under this situation, aerodynamic center of each wing are rotated in the same direction from the original aerodynamic center location with the same amount of the lift force. This will lead to rotation clockwise or counterclockwise. The last one to be considered is the rolling moment. To create the rolling moment, each wing has to have different flapping stroke amplitude. As depicted in Fig. 5.6, one side of wing increase the flapping amplitude and the other side of the wing decrease the flapping amplitude. At the same time, both sides of wings have neutral position about the flapping stroke center line, $\beta = 0^{\circ}$. Consequently, the left-hand wing can create greater amount of lift force than those of the right-hand wing. This imbalanced lift force can rotate the body clockwise.

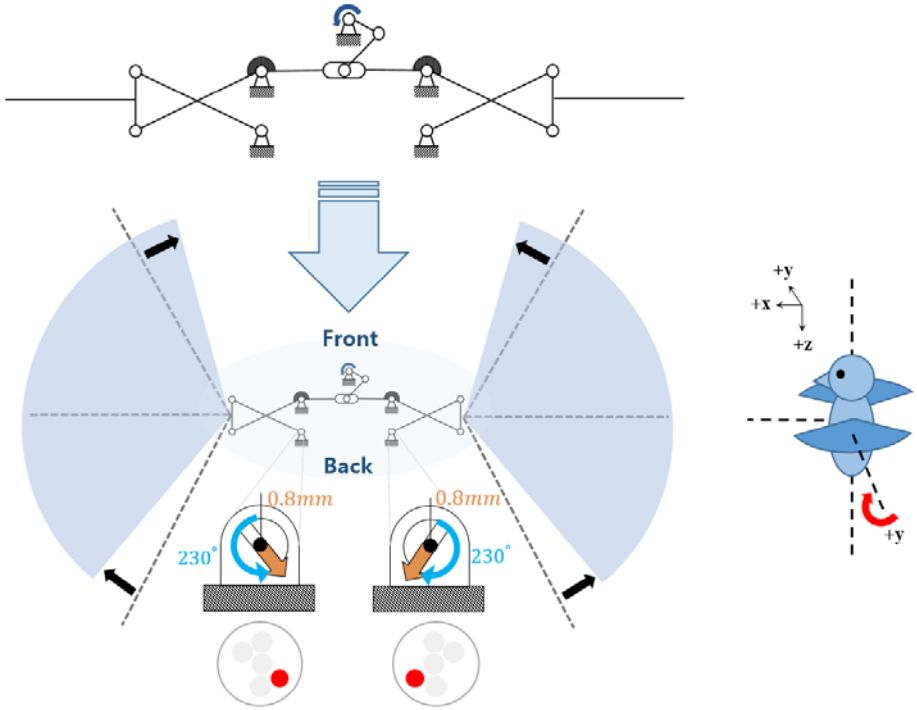

Figure 5.4 Joint position of the pitching motion

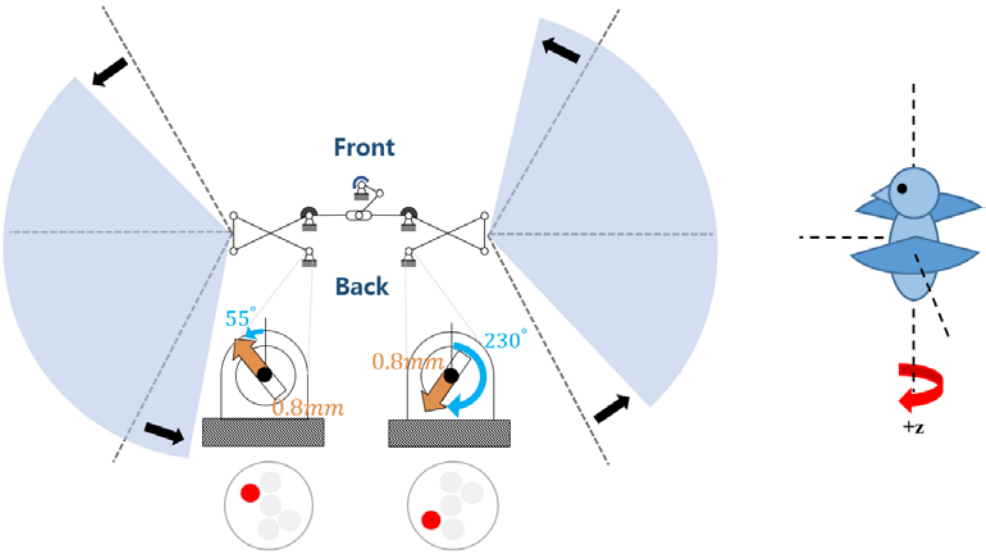

Figure 5.5 Joint position of the yawing motion

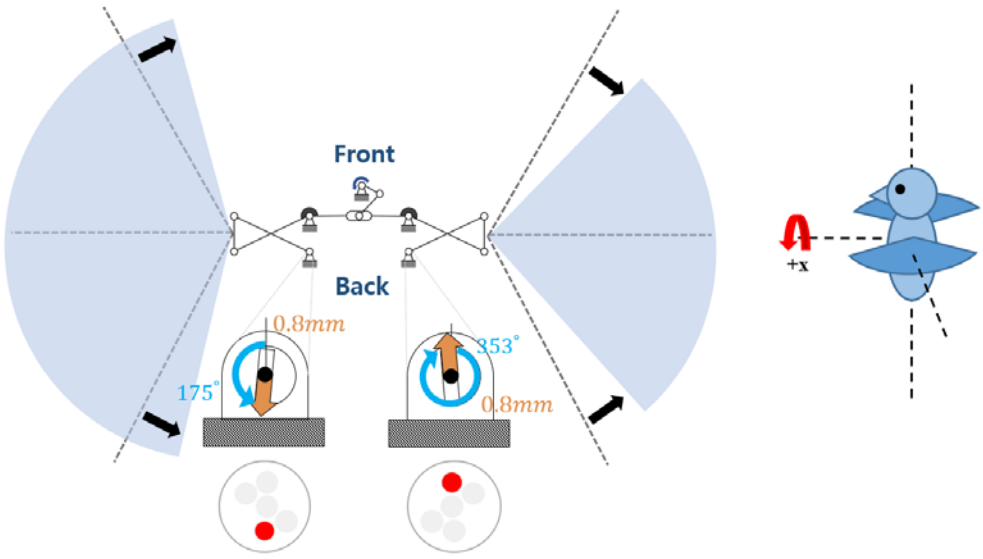

Figure 5.6 Joint position of the rolling motion

VI. Multi-body dynamic analysis

6.1 Flapping mechanism

Before conducting multi-body dynamic analysis for the present mechanism is performed, three-dimensional modeling is created. Based on the kinematic analysis, three-dimensional flapping mechanism is designed as shown in Fig. 6.1. It consists of rivets, DC motor (DiDEL MK07-08), gears, brass bearing, and body frame (Epoxy glass laminate). In the three-dimensional configuration, multiple number of the yellow circular-sectional shaft pins represent fixed the hinge inserted in the body frame. Moreover, those pins mainly withstand the load generated by the flapping motion. The motor and gear box are located below the present mechanism. And those are located between two wings by considering the center of gravity of the whole vehicle. The end of the linkages are designed in order to holding a wing batten connected to the wing membrane. Material of the present body frame is chosen as epoxy glass laminate which is light and structurally strong. Then, the flapping amplitude of the present three-dimensional configuration is estimated by using the multi-body dynamic analysis. To identify the kinematic solution obtained at the conceptual design stage, the analysis is performed by assuming all components as rigid-bodies. As shown in Fig. 6.2, the results obtained by the present mechanism show upstroke and down-stroke having symmetric amplitudes at the constant time step. Thus, the stroke motion is relatively well matched

by sinusoidal graph. Also, the flapping amplitude is estimated to be as sufficient as approximately 160°

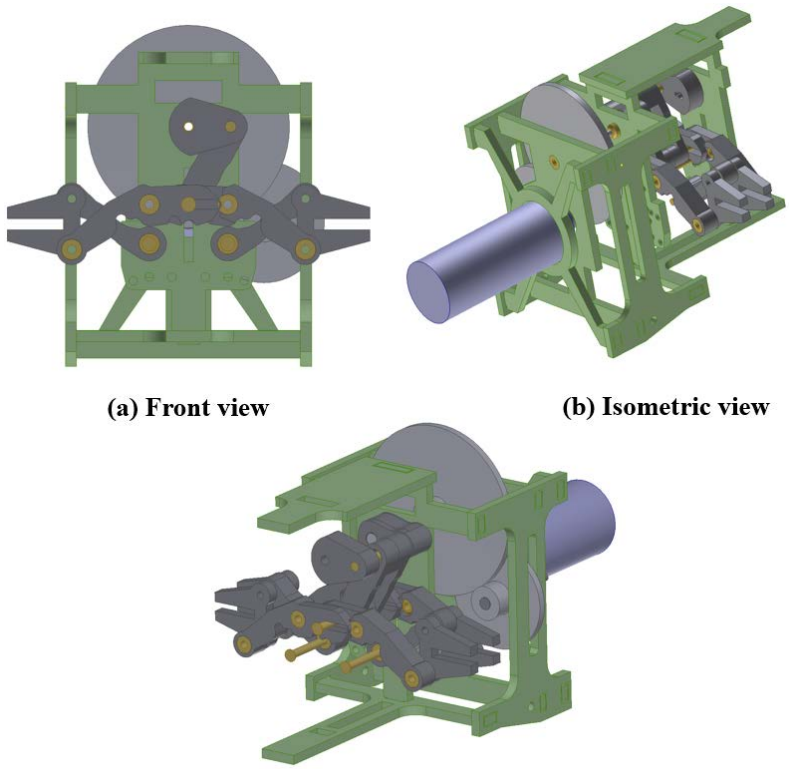

(a) Front view (b) Isometric view

(c) Isometric view

Figure 6.1 Three-dimensional CAD drawings of the present flapping mechanism

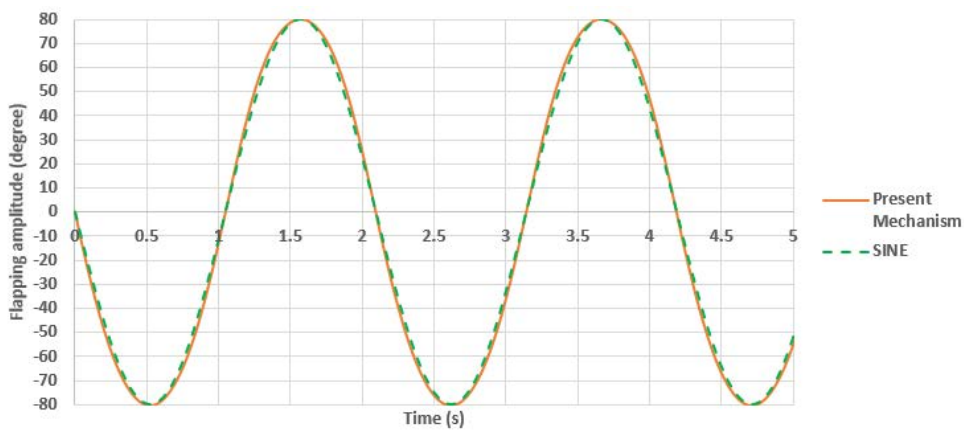

Figure 6.2 Rotation angle of the present flapping wing mechanism

6.2 Control mechanism

The present control mechanism is designed to generate joint motion by obeying the specified manners described previous in Section V. In the present three-dimensional configuration, simple rotating and pulling mechanism is employed to make a control motion as shown in Fig. 6.3. By this structure, the fabrication of control mechanism is simplified. To analyze the present control mechanism, multi-body dynamic analysis, RecurDyn, is used. In Fig. 6.4-(a), the components in blue color are devised to control the flapping stroke by adjusting the θ- rotation. And those in brown color depicted in Fig. 6.4-(b), are devised to control the flapping stroke by adjusting the body along r - direction.

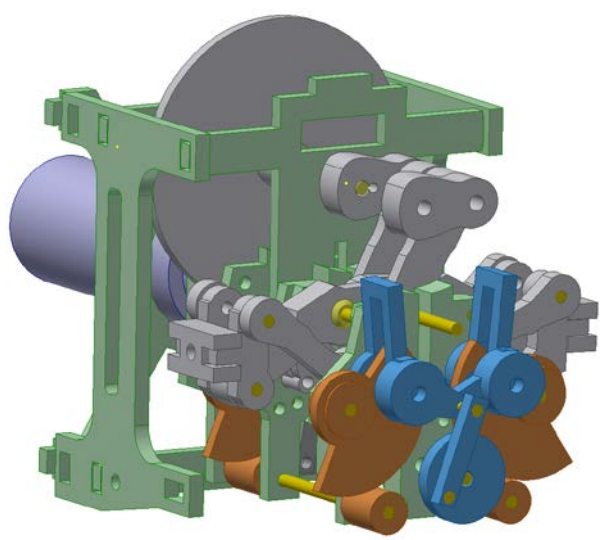

Figure 6.3 Three-dimensional CAD drawings of the present control mechanism

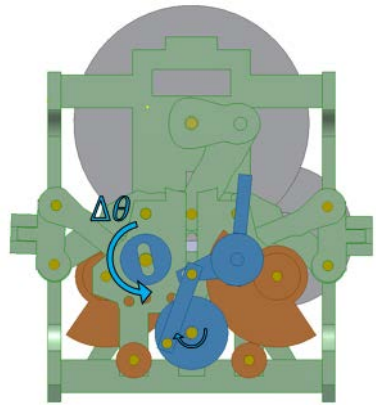

(a) θ - motion

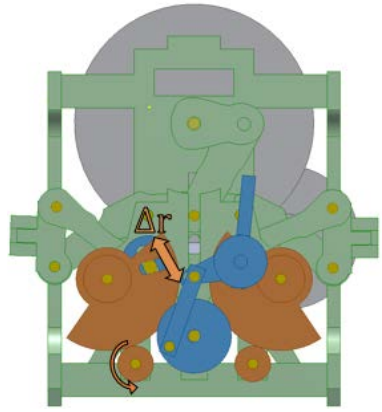

(b) r - motion

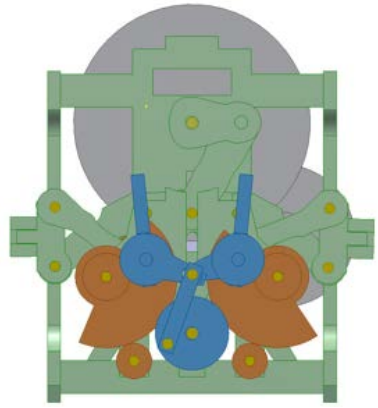

(c) Front view

Figure 6.4 Three-dimensional CAD drawings for the θ, r motions

6.3 Flexible Multi-body dynamic analysis

After the three-dimensional design regarding the flapping and control mechanism is completed, flexible multi -body dynamic (FMBD) analysis is conducted to predict the stress induced in the linkages. In this analysis, the flapping stroke frequency is chosen to be satisfied with the design requirement, 37Hz. The relevant result are illustrated in Fig. 6.5 and Fig. 6.6. The maximum von Mises stress is predicted to be 291MPa in link 1 as shown in red color in Fig. 6.5. Epoxy glass laminate possesses 870MPa for its yield strength. By comparing the maximum predicted stress with the material yield strength, the safety of the present mechanism is proved. However, in the present flexible analysis, flapping operation in vacuum is considered. In order to obtain more realistic result, aerodynamic loads induced by the flapping motion will be predicted and added.

Next, the joint motion is prescribed to change the flapping stroke amplitude α. In this analysis, link 1 and link 5 are modeled as flexible body because they are influenced by relatively high structure load in vacuum condition. The results are shown in Fig. 6.7. When the joint moves along the positive r-direction and rotates in θ by 175°, the flapping amplitude will be increased. On the other hand, when the joint moves in the negative direction of r-direction and rotates in θ by 175°, the flapping amplitude is decreased. In order to generate the yawing motion, the flapping amplitude keeps the same but the flapping plane needs to be rotated. As shown in Fig. 6.8, when the joint moves along the r-direction and rotates in θ by 230°, the flapping average location is increased by approximately 8°. This suggests that the flapping plane will be rotated while sustaining the same flapping amplitude. On the other hand, when joint moves along r-direction and rotates in θ by 55°, the flapping plane will be rotated in an

opposite direction while maintaining the same flapping amplitude. As a result, the preliminary idea of the present control mechanism is significantly improved in a three-dimensional mechanism. And it is found to be possible to generate the pitching, rolling, and yawing motions by using the present design.

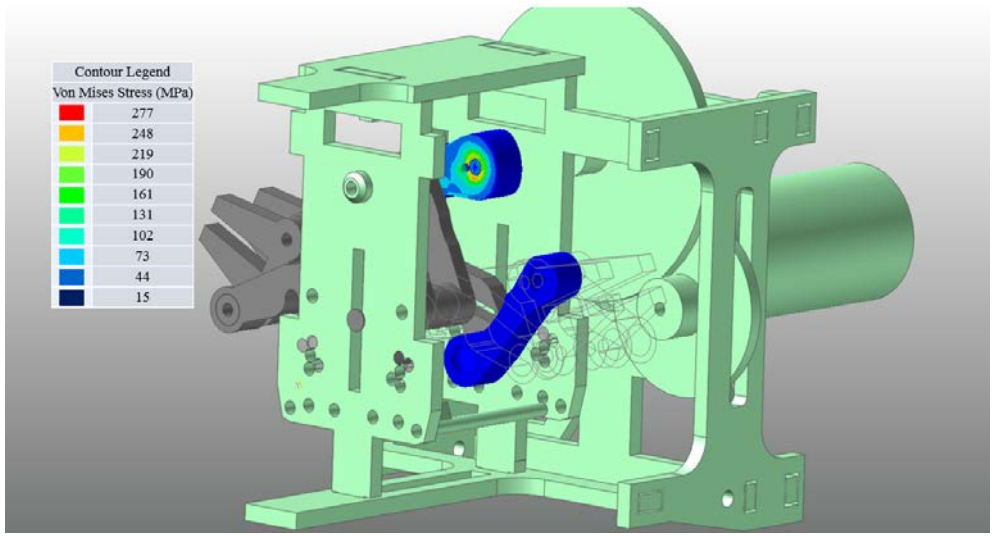

Figure 6.5 Stress contour about Link 1 predicted by RecurDyn

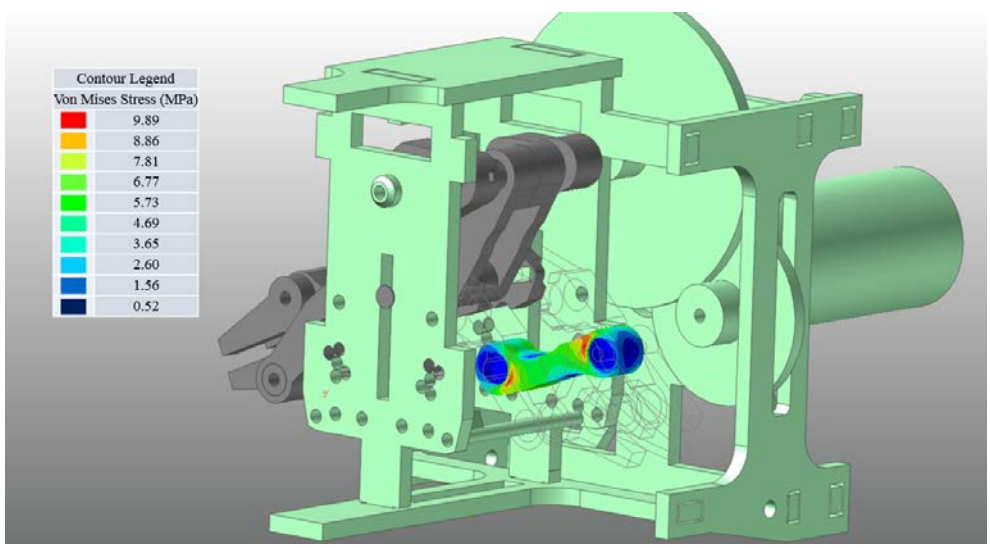

Figure 6.6 Stress contour about Link 5 predicted by RecurDyn

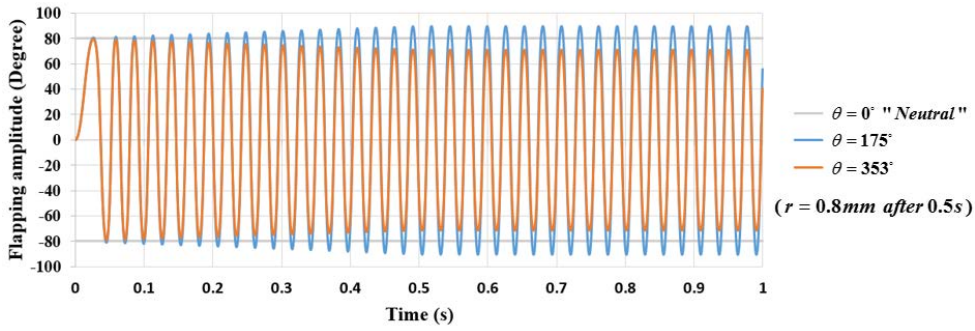

Figure 6.7 Flapping amplitude variation according to θ- and r- direction joint

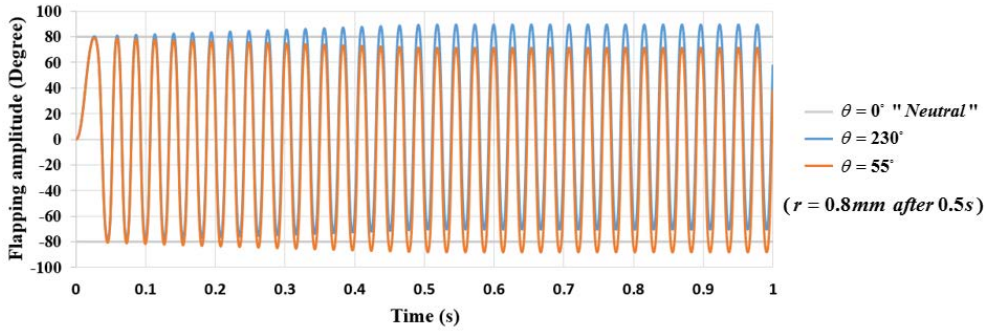

Figure 6.8 Flapping amplitude variation according to θ- and r- direction joint

VII. Fabrication and Experiment

7.1 Fabrication

Figure. 7.2 shows the presently fabricated prototype. Figure 7.3 is side view. To satisfy the design requirement, body components are made by epoxy glass laminate having high rigidity and being relatively light when it is compared with other materials. The plates with the thickness as 1 mm and 2 mm are cut by CNC cutting machine for body components. In all connected joints, the brass bearing having 0.8 mm-diameter are used to maintain accuracy and minimize the rotational friction. Motor is selected to be MK07-08 from DiDEL. It can generate 0.37 N-mm and 48,000 rpm in no load condition with 5V. And then, 12/36 teeth gear and 12/60 teeth gear by DiDEL are used in order to obtain the 20:1 gear ratio. Using this gear ratio, motor has 7.4 N-mm torque and 2.400 rpm with no load condition in 5V. This condition is set to satisfy the present flapping frequency, 37Hz. Consequently, the external dimension of the driving component is $25 \times 26 \times 30.2$mm and the gross weight is 8.3g except the battery. Flapping wing has 150mm of the wingspan and its wing membrane is made by polyethylene with 15 micron thickness as shown in Fig. 7.1 [2]. To support the wing, 1 mm carbon rods are used for a leading edge of each wing. The membrane is not adhere to carbon rod, however it encloses the rod. Thus, during the flapping motion, the wing membrane rotates feely and passively along the leading edge due to the inertia load of the wing.

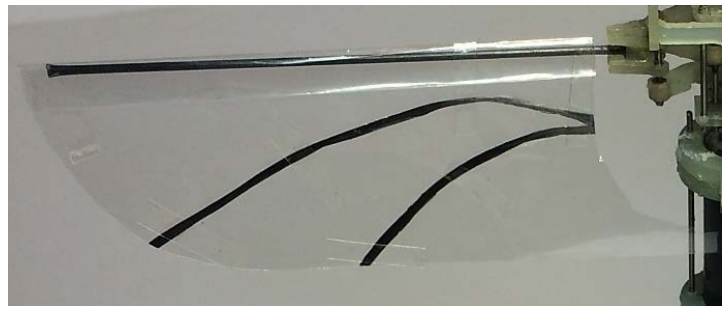

Figure 7.1 Fabricated prototype of the wing

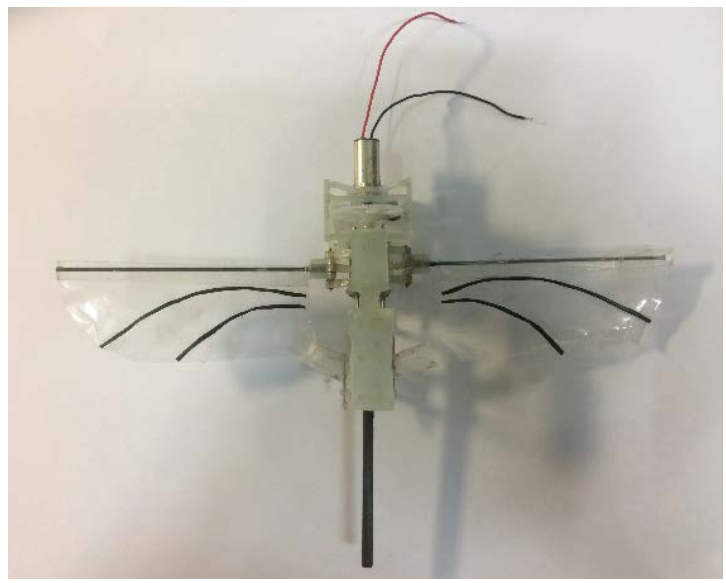

Figure 7.2 Fabricated prototype

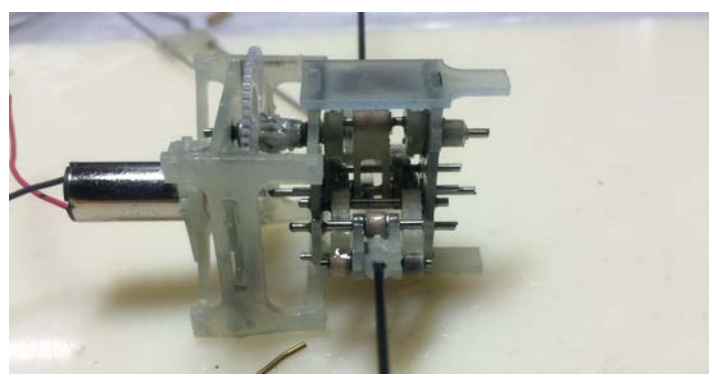

Figure 7.3 Side view of the assembled prototype

7.2 Experiment

Using the fabricated prototype, the flapping wing trajectory of the wing is examined. The trajectory is measured by using the high speed camera Micro M100 by Phantom. In the test, the input voltage for supplying power is 5V. The resulting flapping frequency is 25Hz. The present mechanism is fixed on the experimental mount, as shown in Fig. 7.4. The first condition is the neutral condition as shown in Fig. 7.5-(a). The flapping trajectory is seemed to be symmetric and the relevant flapping amplitude, α, is approximately 160°. Then, by following each joint location, three cases for pitching, rolling and yawing motions are examined. The position of each joint is based on the specified manners described in Section V-B.

The second condition is pitching motion. The centerline of the both wings is rotated symmetrically by 8°. This motion matches well with the analytical solution, as shown in Fig. 7.5-(b). The third condition is the rolling motion. For the rolling motion, from the analytical estimation, the flapping amplitude of the one side of the wing is predicted as 176° and the other side of the wing is predicted as 144°. As shown in Fig. 7.5-(c), the presently fabricated mechanism matched well with the experiment results. The last condition is the yawing motion. It also shows good agreement with the analytical solution, as shown in Fig 7.5-(d). In all the conditions, there exist approximately $\pm 3^{\circ}$ differences between the analytic solution and the experiment results. There may be several reasons for such differences. The first possible reason is that in the actual

experiment there exist additional aerodynamic force on the wing surface but it is not considered in multi-dynamic analysis. The second reason is that there exist manufacturing inaccuracy which is generated by CNC cutting machine or abrasion in the fabrication procedures.

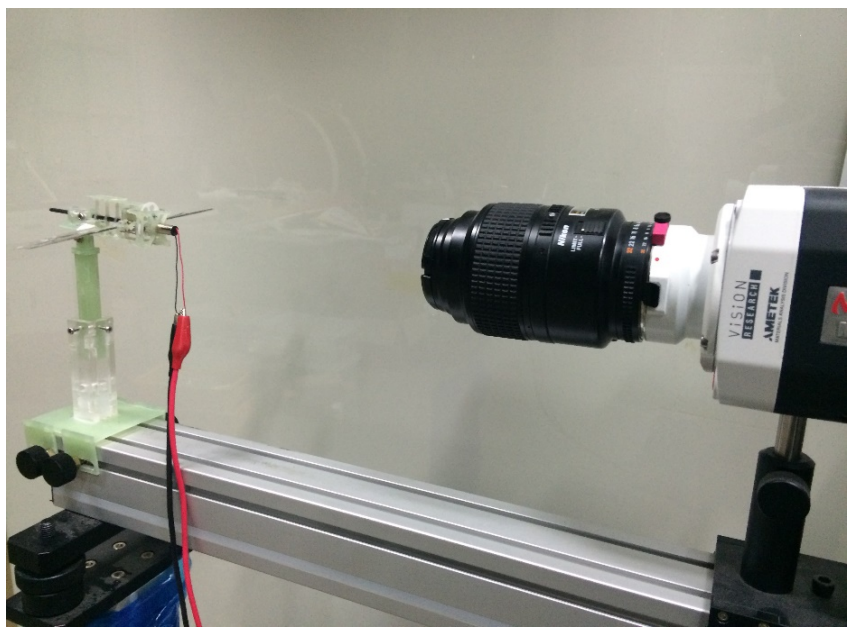

Figure 7.4 Flapping motions captured by the high-speed camera

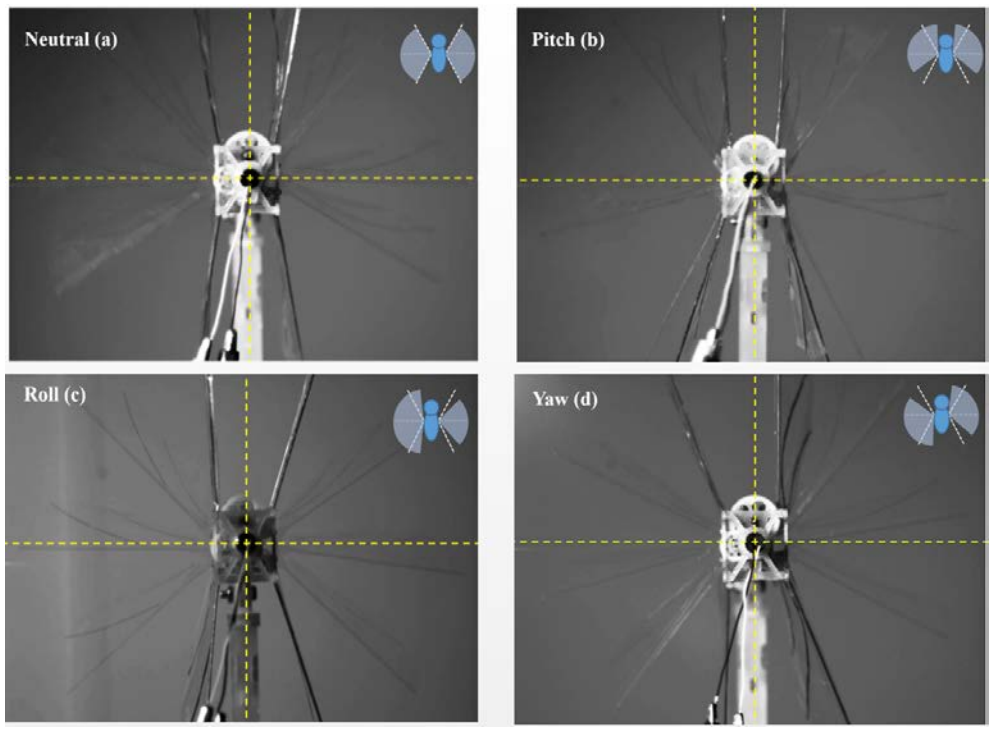

Figure 7.5 Presently fabricated prototype

FWMAV needs to change their wing aerodynamic force in order to control their position or their body attitude. In order to examine the FWMAV`s control capability, a test bed is prepared. Nano-17, load cell by ATI is used to measure the 6-axis load force component which is generated by the present wing kinematic modification. Experimental mount, which has three degrees of freedom, is designed. It can trim the body posture to obtain a more precise result. Moreover, it is connected between load cell and flapping mechanism. Figure 7.7 shows the results of the measured loads which generated by the present flapping mechanism. All the curves are smoothed by applying the low-pass filter (cut-off frequency 25Hz). Figure 7.7 represents the lift. The average value of the measured vertical loads is 0.141N. It means that the takeoff weight of the designed present mechanism is 14.4g. Because the present driving component weights 8.3g, flapping mechanism is expected to be capable of taking off. Figure 7.8 shows the pitching moment in + direction. The measured average pitching moment is 0.459 N-mm. Next is the rolling moment in + direction. The generated rolling moment is 0.7 N-mm as shown in Fig. 7.9. This value also provides the average rolling moment. The last quantity is the yawing moment. In the yawing motion, both wings are rotated in the same direction either clockwise or anticlockwise. By this motion, yawing moment is generated. The average value of yawing moment is obtained to be 0.272 N-mm, as shown in Fig. 7.10. By this experiment, the amount of the control forces and moments generated by the present flapping mechanism are measured and examined. As a result, it is confirmed that such control forces and moments will be sufficient for changing the body posture of the present vehicle.

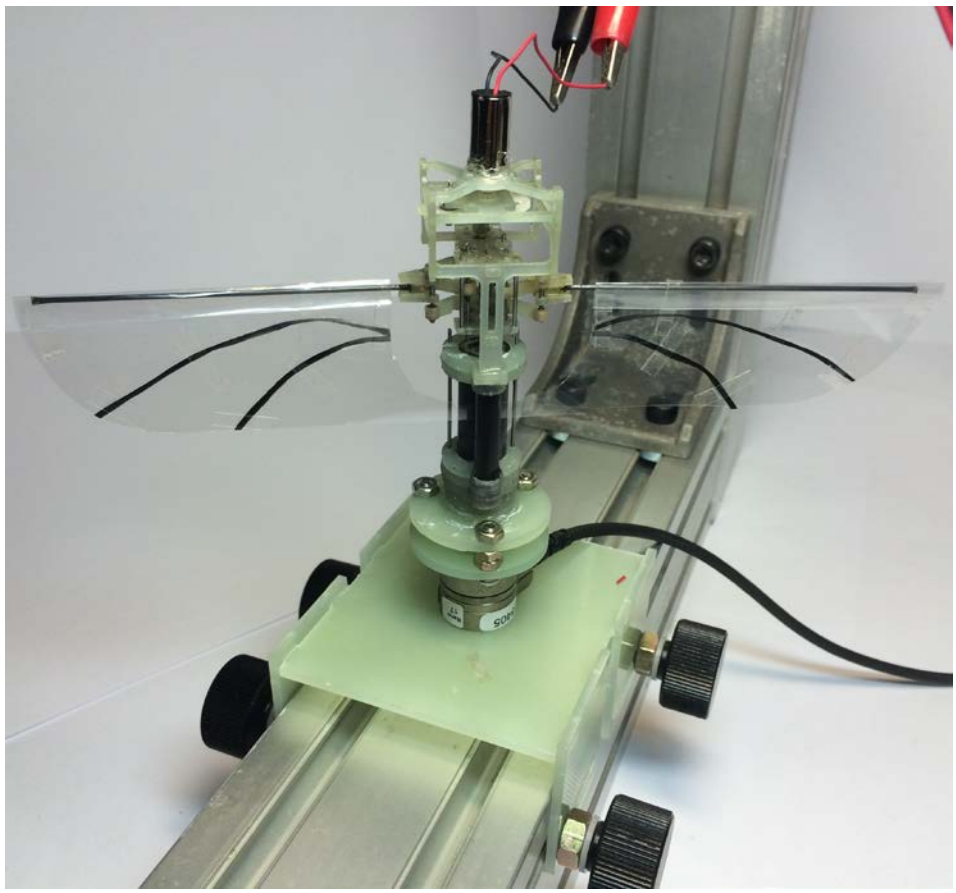

Figure 7.6 Presently fabricated test bed and the load cell

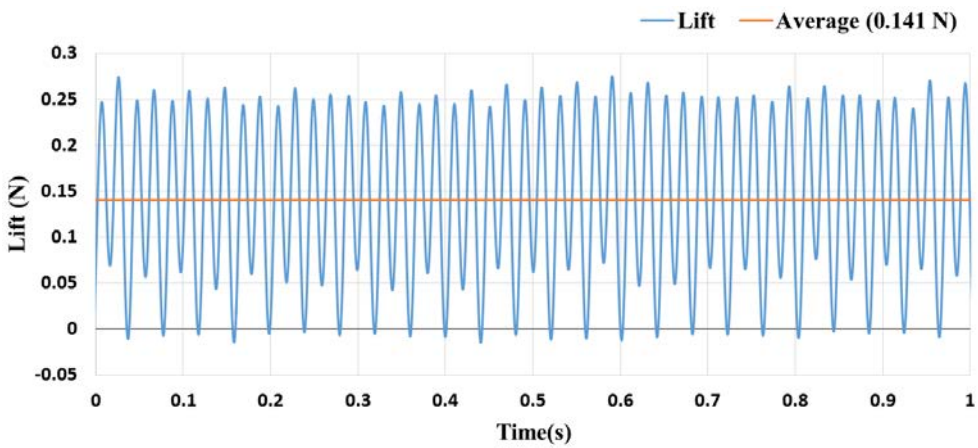

Figure 7.7 Measured Lift

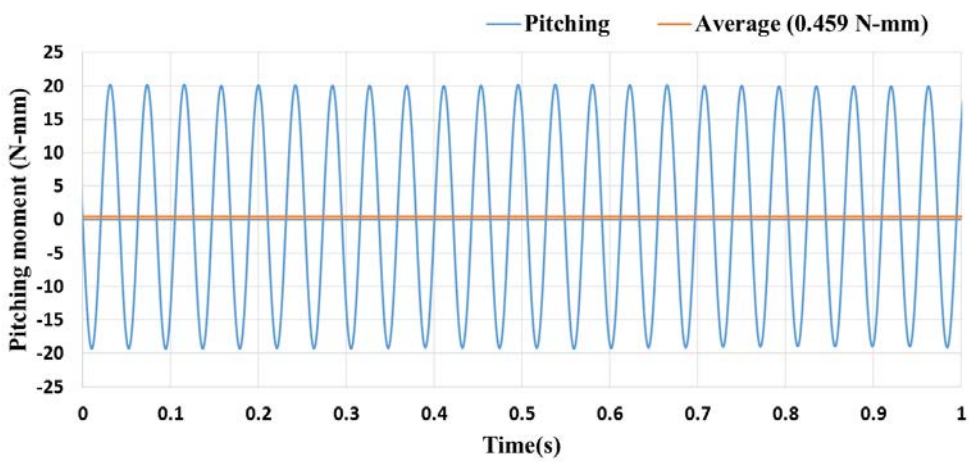

Figure 7.8 Measured pitching moment

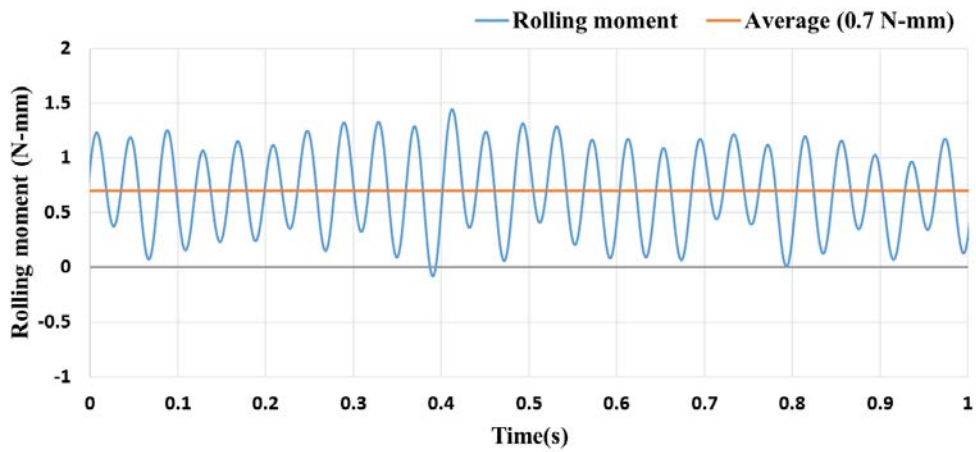

Figure 7.9 Measured rolling moment

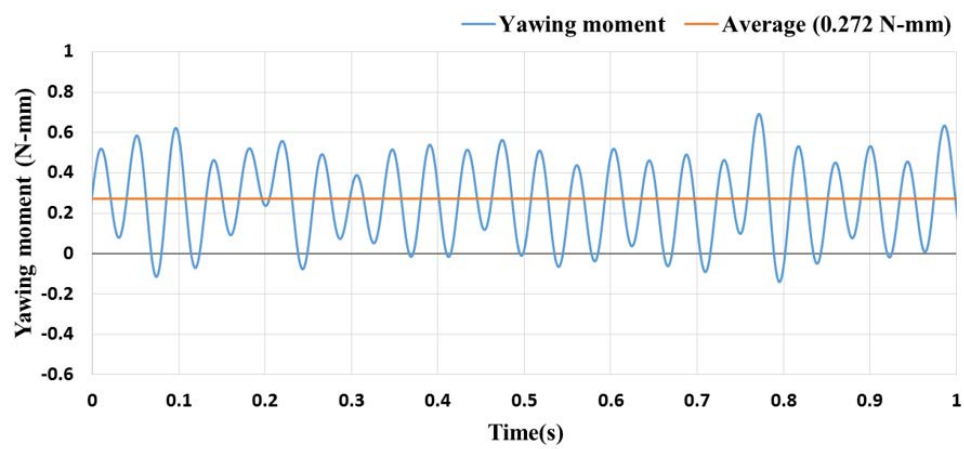

Figure 7.10 Measured yawing moment

VIII. Conclusion and Future Works

8.1 Conclusion

In this thesis, according to the design procedure, a new FWMAV using six-bar linkage is introduced. First, several design requirements are established by using UBET for appropriate FWMAV`s ability. And obeying the FWMAV requirements, detail design is performed. Six-bar linkage is used for flapping mechanism and it shows a sufficient flapping stroke amplitude, approximately 160°. Then, control mechanism is considered to generate flight control moments for pitching, yawing and rolling motion by modifying the wing`s kinematics, such as flapping amplitude, rotation of the flapping center line. This control motion is implemented by joint motion. The change of the flapping amplitude is made by size displacement of joint. Then, three-dimensional model is designed to consider the real parts and materials. Moreover, to ensure the performance of the present design, multi-body dynamic analysis using RecurDyn is conducted. In the analysis, flapping amplitude is predicted to be approximately 160°. Control motion for changing the wing kinematics is also predicted by considering the joint motion with respect to the variations of the joint motion. Last, the performance of the present design is evaluated by experiment. Wing`s trajectory are captured by high speed camera. By this procedure, it is possible to estimate mechanism performance considering aerodynamic force and also fabrication error. The results are well matched by kinematic analysis within $\pm 3^{\circ}$. And then, the experiment using the load cell is conducted to evaluate whether the generated moments are proper to change

the vehicle attitude or not. Measured pitching, rolling and yawing moments show the possibility of the control capability about designed mechanism

8.2 Future works

There existed limit to fabricate the present concept because internal and external factors are not considered. Thus, flexible multi-body dynamic analysis is additionally performed by considering aerodynamic loads induced by the wing motion. To predict such aerodynamic loads accurately, VLM or CFD will be employed. And such predicted aerodynamic loads will be applied for the multi-body analysis. As a result, the detail design of the present FWMAV will be improved and the three-dimensional CAD drawings will be obtained.

The flapping frequency in the present mechanism is 25 Hz. It is lower than the design requirement, 37Hz. The reasons are that there exist frictions between links, fabrication error and large inertia on each link. To solve these problems, links shape need to be changed for small inertia and more accurate fabrication process.

The control mechanism is not fully designed for the automatic system. To do this, the mechanism is need to be designed with the servo motors. And also, it have light and robustness to reliability

Reference

[1] Keenon, M., Klingebiel, K., Won, H, and Andriukov, A., "Development of the Nano Hummingbird: A Tailless Flapping Wing Micro Air Vehicle", 50th AIAA Aerospace Sciences Meeting including the New Horizons Forum and Aerospace Exposition, January, 2012.

[2] Truong, T. Q., Phan, V. H., and Park, H. C., "Effect of Wing Twisting on Aerodynamic Performance of Flapping Wing System", AIAA Journal, Vol. 51, No. 7, July, 2013.

[3] Teoh, Z. E., Fuller, S. B., Chirarattananon, P., Prez-Arancibia, N. O., Greenberg, J.D., and Wood, R. J., "A Hovering Flapping-Wing Micro robot with Altitude Control and Passive Upright Stability", IEEE/RSJ International Conference on Intelligent Robots and Systems, October 7-12, 2012.

[4] Yang, L.-J., "The Micro-Air-Vehicle Golden Snitch and Its Figure-of-8 Flapping", Journal of Applied Science and Engineering, Vol. 15, No. 3, pp. 197-212, 2012.

[5] Gaissert, N., Mugrauer, R., Mugrauer, G., Jebens, A., Jebens, K., and Knubb, E. M., "Inventing a Micro Aerial Vehicle Inspired by the Mechanics of Dragonfly Flight", Lecture Notes in Computer Science, pp. 90-100, 2014.

[6] Karasek, M., Nan, Y., Lalami, M., Preumont, A., "Pitch moment generation and measurement in a robotic hummingbird", nternational Journal of Micro Air Vehicles, pp. 299–309, 2013.

[7] Teng, N.H., "The development of a computer code (U2DIIF)--for the numerical solution of unsteady," Naval Postgraduate School, June, 1987.

[8] Nguyen, Q. V., Park, H. C., Byun, D. Y., Goo, N. S., “Recent progress in developing a beetle-mimicking flapping-wing system”, World Automation Congress (WAC), pp.1-6, 2010.

[9] Groen, M., Bruggeman, B., Remes, B., Ruijsink, R., Van Oudheusden, B. W., & Bijl, H., “Improving flight performance of the flapping wing MAV DelFly II”, In Int. Micro Air Vehicle Conf. and Competition (IMAV 2010)

[10] Festo, A. G., "BionicOpter", 2013.

[11] Anonymous, RecurDyn User’s Manual, FunctionBay, Inc., 2012.

국문초록

6 절 링크를 이용한 날갯짓 초소형 비행체 설계

전 재 혁

기계항공공학부

서울대학교 대학원

과거부터 자연계 날갯짓 운동을 하는 생물체에 대한 연구가 활발히 진행되어 왔으나 지금까지 설계단계에서 실제적인 기구학적 해석을 진행 적용한 사례가 거의 없었다. 본 논문에서는 초소형 비행체의 날갯짓 운동 메커니즘과 제어 메커니즘을 설계를 진행하였고, 설계단계에서 설계안의 정확성을 미리 확보하고자 기구학적 해석을 진행하였다. 설계 목표는 unsteady blade element theory (UBET)와 해석적인 방법을 통해 정립되었다. 설계한 날갯짓 메커니즘은 6 절 링크를 기반으로 양쪽 날개에 배치되어 구동부 크기, 날갯짓 각도, 등의 설계 목표를 만족 하도록 고안되었고, 제어 메커니즘은 링크절 조인트의 위치변화를 통하여 모멘트를 변화를 발생하도록 고안되었다. 계산된 날갯짓의 거동에 따라 각 링크의 구성요소를 3 차원 형상으로 설계하였고 날갯짓 메커니즘과 제어 메커니즘의 개략적인 거동의 가능성과 그 특징의 분석은 다물체 동역학 해석 프로그램인 RecurDyn 을 이용하여 수행하였다. 그런 뒤, 실제 제작과 실험을 통하여 설계안의 날갯짓 속도, 날갯짓 궤적, 공력 등의 성능을 확인 하였다. 향후 개념설계를 기반으로 공력하중을 추가 고려한 실제적 해석을 진행하고 설계에 적용할 계획이다.

주요어 : 날갯짓 비행체, 다물체 동역학, 6 절 링크

학 번 : 2014 - 20667